Inorg. Chem. **2008**, *47*, 8543−8552

Forum

Target-Aimed Synthesis of Anion-Deficient Perovskites

Evgeny V. Antipov, Artem M. Abakumov,* and Sergey Ya. Istomin

Department of Chemistry, Moscow State University, Moscow 119991, Russia

Received April 30, 2008

The brownmillerite-type $A_2B_2O_5$ structure is considered as a parent one, giving rise to different derivatives: layered double perovskites, A-site and anion-vacancy-ordered perovskites, and the perovskite-like compounds with crystallographic shear planes. The structural relationships and synthesis pathways for these classes of materials are discussed with particular attention to the ordering at the A or B sublattices, anion vacancy ordering, and their mutual interaction.

1. Introduction

Anion-deficient perovskites $ABO_{3-\delta}$ have attracted the attention of the scientific community because of their diverse physical properties, e.g., high-T_c superconductivity in Cu-based mixed oxides, mixed high electron and oxygen ion conductivity, and rich magnetic behavior, which make them promising materials for various applications. These properties are strongly influenced by cation and anion ordering often present in their structures. The purpose of this contribution is to draw attention to new pathways toward perovskite structures with ordering at A, B, and/or anion sublattices. Obtaining a perovskite-like compound with a requested ordering type is often a challenging task. Especially it concerns the structures that are too demanding of the crystal chemistry properties of the constituting elements, such as perovskites with a layered arrangement of B cations, where the ordering can be achieved only for cations whose charge and size differences lie in a narrow range. The brownmillerite $A_2BB'O_5$ structure is considered here as the parent structure, which can be appropriately modified using extra anion insertions, heterovalent replacement at the A sublattice, or insertion of the A cation with a lone electron pair. Particular attention is devoted to a delicate interplay of the ordering at the A or B sublattices and the anion vacancy ordering and to the effects of their mutual stabilization. Application of these approaches is discussed using examples of layered double perovskites, A-site and anion-vacancy-ordered perovskites, and the perovskite-like compounds with crystallographic shear planes.

2. Brownmillerite Structure and Layered Ordering of B Cations

Among anion-deficient perovskites, $ABO_{2.5}$ (or $A_2B_2O_5$, $A_2BB'O_5$, and $AA'B_2O_5$, where A, A′, B, and B′ are cations of different kinds) are, perhaps, the most prevalent and rich in structural variety. Generally, O atoms are removed from the perovskite structure along the $[100]_p$ or $[110]_p$ rows or in the $(001)_p$ planes,[1] which for $ABO_{2.5}$ corresponds to removal in an ordered way of 25% of $[100]_p$ or $[110]_p$ oxygen rows or to a complete removal of O atoms from 50% of the AO layers. In all cases, ordering of O atoms and vacancies reduces the coordination number of the B cations and the structure can be alternatively considered as an ordered pattern of the defect BO_{6-x} polyhedra. The exact pattern depends on several factors, such as the presence of the cations with distinct crystallographic properties at the A and/or B sublattices, and the valent state of the B cations. The $t_{2g}^3e_g^1$ or $t_{2g}^6e_g^3$ electronic configuration of the B cation (Mn^{3+} or Cu^{2+}) favors the oxygen removal along the $[100]_p$ rows or in the $(001)_p$ planes that transforms the BO_6 octahedra to BO_5 tetragonal pyramids and finally to BO_4 squares (characteristic for Cu^{2+} rather than for Mn^{3+}).[2] An extra energy gain due to the Jahn−Teller effect additionally promotes such

* To whom correspondence should be addressed. E-mail: abakumov@icr.chem.msu.ru. Tel: +7 (495) 939-52-44. Fax: +7 (495) 939-47-88.

(1) Anderson, M. T.; Vaughey, J. T.; Poeppelmeier, K. R. *Chem. Mater.* **1993**, *5*, 151–165.
(2) Hadermann, J.; Van Tendeloo, G.; Abakumov, A. M. *Acta Crystallogr.* **2005**, *A61*, 71–92.

10.1021/ic800791s CCC: $40.75
Published on Web 09/29/2008

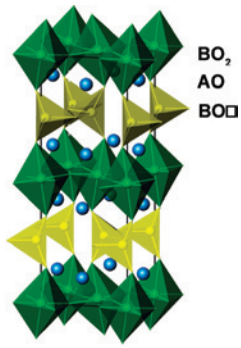

Figure 1. Crystal structure of the $A_2B_2O_5$ brownmillerite. The B cations are situated in the octahedra and tetrahedra, and the A cations are shown as spheres.

Table 1. Equatorial and Apical B−O (B = Cu, Fe, In) Bond Lengths in the BO_6 Octahedra in Brownmillerites

composition	d(B−O_{eq}), Å	d(B−O_{ap}), Å	reference
$LaCaCuGaO_5$	1.916−1.922	2.406	5, 6
$RSrCuGaO_5$ (R = La, Pr, Nd)	1.731−2.112	2.407−2.494	7, 8
$Ca_2Fe_2O_5$	1.957−1.980	2.114−2.162	9−13
$Sr_2Fe_2O_5$	1.940−2.028	2.202−2.217	14, 15
Ca_2AlFeO_5	1.942−1.954	2.217	16
Ca_2GaFeO_5	1.954−1.959	2.128	17
$Ba_2In_2O_5$	2.136	2.315	18

oxygen vacancy ordering. An ability of the B cation to adopt a stable tetrahedral environment is favorable for the $[110]_p$ oxygen vacancy rows. Vacant and oxygen-filled $[110]_p$ rows alternate along the $[\bar{1}10]_p$ direction, resulting in the chains of corner-sharing $B'O_4$ tetrahedra and the $B'O\square$ ($\square$ = oxygen vacancy) composition of the anion-deficient layers. Alternation of the BO_2 and $B'O\square$ layers along the $[001]_p$ axis results in a brownmillerite-type structure $A_2BB'O_5$, where the B cations residing in the BO_2 layers retain the octahedral coordination (Figure 1). The brownmillerite-type ordering can be realized when the B positions are occupied by cations, which are able to adopt equally octahedral and tetrahedral coordination. The brownmillerite $A_2B_2O_5$ (A = Ca, Sr, Ba) structure is common for the trivalent cations with the spherically symmetric valent elecronic shell, such as Fe^{3+} or In^{3+}, where there is no significant energy difference between the octahedral and tetrahedral coordination according to the crystal-field theory. In the $A_2BB'O_5$ brownmillerites with two types of the cations B and B′, the ordering of anion vacancies occurs concomitantly with the B and B′ cation ordering and both are of the layered nature. The preference of the cations toward either octahedral or tetrahedral coordination plays the major role in their ordering, whereas parameters such as charge and size difference, crucial for the cation ordering in the $A_2BB'O_6$ double perovskites,[3] are of secondary importance. Another factor stabilizing the brownmillerite-type ordering is the electronic configuration of the octahedrally coordinated B cation, which favors apically elongated octahedron due to the Jahn−Teller effect. Indeed, a combination of the tetrahedral and octahedral sites as in the brownmillerite structure provides an excellent host for the octahedrally coordinated Jahn−Teller active B cations.[4] The BO_6 octahedra are apically elongated in many

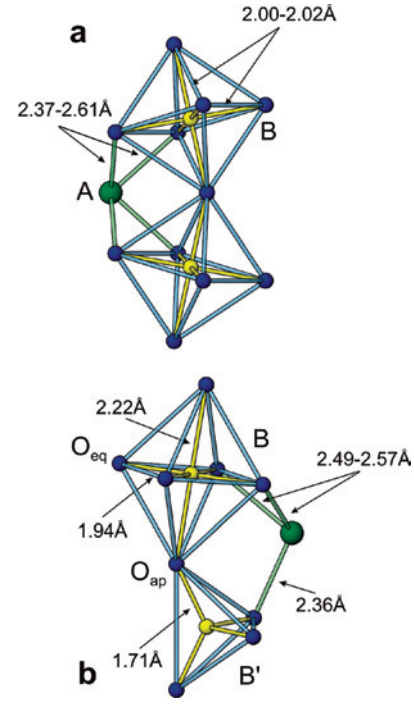

Figure 2. Fragments of the $NdFeO_3$ perovskite (a) and Ca_2AlFeO_5 brownmillerite (b) structures with the most relevant bond lengths.

brownmillerites, giving four short in-plane equatorial B−O_{eq} bonds and two longer apical B−O_{ap} bonds, as was found, for example, in Cu^{2+}-based compounds (see Table 1). However, the Jahn−Teller effect is not the primary cause of the apical elongation of the BO_6 octahedra in brownmillerites. The short metal−oxygen bonds for the B′ cations in the tetrahedra also require this apical elongation in order to keep an appropriate separation between the octahedral and tetrahedral layers and reasonable distances between the A cations and the neighboring O atoms. In the fragments of the perovskite $NdFeO_3$[19] and brownmillerite Ca_2AlFeO_5[16] structures (Figure 2), the octahedral coordination environment

(3) Anderson, M. T.; Greenwood, K. B.; Taylor, G. A.; Poeppelmeier, K. R. *Prog. Solid State Chem.* **1993**, *22*, 197–233.
(4) Hadermann, J.; Abakumov, A. M.; D'Hondt, H.; Kalyuzhnaya, A. S.; Rozova, M. G.; Markina, M. M.; Mikheev, M. G.; Tristan, N.; Klingeler, R.; Büchner, B.; Antipov, E. V. *J. Mater. Chem.* **2007**, *17*, 692–698.
(5) Kharlanov, A. L.; Bryntse, I.; Antipov, E. V.; Luzikova, A. V. *Acta Chem. Scand.* **1993**, *47*, 434–438.
(6) Luzikova, A. V.; Kharlanov, A. L.; Antipov, E. V.; Müller-Bushbaum, Hk. *Z. Anorg. Allg. Chem.* **1994**, *620*, 326–328.
(7) Vaughey, J. T.; Wiley, J. B.; Poeppelmeier, K. R. *Z. Anorg. Allg. Chem.* **1991**, *598*, 327–338.
(8) Roth, G.; Adelmann, P.; Knitter, R.; Massing, S.; Wolf, Th. *J. Solid State Chem.* **1992**, *99*, 376–387.
(9) Colville, A. A. *Acta Crystallogr.* **1970**, *B26*, 1469–1473.
(10) Berggren, J. *Acta Chem. Scand.* **1971**, *25*, 3616–3624.
(11) Berastegui, P.; Eriksson, S.-G.; Hull, S. *Mater. Res. Bull.* **1999**, *34*, 303–314.
(12) Redhammer, G. J.; Tippelt, G.; Roth, G.; Amthauer, G. *Am. Mineral.* **2004**, *89*, 405–420.
(13) Krüger, H.; Kahlenberg, V. *Acta Crystallogr.* **2005**, *B61*, 656–662.
(14) Greaves, C.; Jacobson, A. J.; Tofield, B. C.; Fender, B. E. F. *Acta Crystallogr.* **1975**, *B31*, 641–646.
(15) Schmidt, M.; Campbell, S. J. *J. Solid State Chem.* **1999**, *156*, 292–304.
(16) Colville, A. A.; Geller, S. *Acta Crystallogr.* **1971**, *B27*, 2311–2315.
(17) Arpe, R.; von Schenck, R.; Müller-Buschbaum, Hk. *Z. Anorg. Allg. Chem.* **1974**, *410*, 97–103.
(18) Berastegui, P.; Hull, S.; Garcia-Garcia, F. J.; Eriksson, S.-G. *J. Solid State Chem.* **2002**, *164*, 119–130.
(19) Strel'tsov, V. A.; Ishizawa, N. *Acta Crystallogr.* **1999**, *B55*, 1–7.

for the Fe^{3+} cations has a significantly different geometry. In the $NdFeO_3$ orthorhombically distorted stoichiometric perovskite, the apical and equatorial Fe−O bond lengths are almost equal. In the Ca_2AlFeO_5 brownmillerite, the decrease of the metal−oxygen bond lengths for the tetrahedrally coordinated B′ = Al cation requires a shift of the apical O atom away from the Fe cation, for which the Jahn−Teller distortion does not occur due to the d^5 electronic configuration. In Fe- and In-containing brownmillerites, the difference between the equatorial and apical B−O bond lengths is quite remarkable (Table 1). If B is a Jahn−Teller active cation, the coinciding geometric and electronic requirements should ease the formation of the brownmillerite structure. Indeed, a family of the brownmillerite-type compounds is known not only for Cu^{2+} ($t_{2g}^6e_g^3$) but also for another Jahn−Teller active B-cation Mn^{3+} ($t_{2g}^3e_g^1$): $A_2B'MnO_5$, A = Ca, Sr and B′ = Al, Ga.[20−25]

The synthesis conditions for brownmillerites containing transition metals with variable oxidation states should be optimized in order to keep the required valence for the transition-metal cations as well as the anion deficiency. Increasing the oxygen content above the $A_2BB'O_5$ composition will likely destroy the long-range ordering of the B and B′ cations. The R_2MnGaO_6 (R = La, Nd)[26] and $La_{2-x}Sr_xMnGaO_6$ ($x = 0.7$)[27,28] compounds possess distorted disordered perovskite structures. Changing the B:B′ = 1:1 stoichiometric ratio also prevents the formation of the layered brownmillerite structure. The $SrMn_{1-x}Ga_xO_{3-\delta}$ ($0 \le x \le 0.33$) solid solutions have a disordered cubic perovskite structure.[29]

3. From Brownmillerites to Layered Perovskites

The $A_2BB'O_5$ brownmillerites can be considered as anion-deficient analogues of the $A_2BB'O_6$ double perovskites with a layered ordering of the B and B′ cations. One should note that the layered 1:1 ordering at the B sublattice is quite rare and was observed up to now in a limited number of perovskites $R_2CuB'O_6$, where R = La, Nd, Pr, Sm and B′ = Sn^{4+}, Zr^{4+}.[30,31] The CuO_6 octahedra demonstrate remarkable apical elongation in these compounds ($\langle d(Cu-O_{eq})\rangle = 1.99$ Å and $\langle d(Cu-O_{ap})\rangle = 2.38$ Å in La_2CuSnO_6), whereas the SnO_6 octahedra are slightly apically compressed ($\langle d(Sn-O_{eq})\rangle = 2.07$ Å and $\langle d(Sn-O_{ap})\rangle = 2.02$ Å). It is assumed that the layered ordering is stabilized when the charge difference between the B and B′ cations is 2 and the Jahn−Teller cation B smaller than the B′ cation is by 0.08−0.12 Å.[3] Deviations from these criteria result in a disordered placement of the B and B′ cations. The perovskites $CaRMnSnO_6$ (R = La, Pr, Nd, Sm−Dy) (charge difference 1)[32] and R_2MnGaO_6 (R = La, Nd) (charge difference 0)[26] are characterized by the orthorhombic $GdFeO_3$ structural type, with the Mn^{3+} and Sn^{4+} (Ga^{3+}) cations randomly occupying the octahedral sites. The family of layered double perovskites can be significantly extended if the following synthesis strategy is applied: (1) preparation of the brownmillerite-type anion-deficient $A_2BB'O_5$ perovskite where the layered ordering of the B and B′ cations is promoted by ordering of oxygen vacancies due to their different favorable oxygen coordination and can be additionally stabilized by a Jahn−Teller distortion of the BO_6 octahedron; (2) low-temperature oxidation of the $A_2BB'O_5$ brownmillerite at the conditions preserving the layered ordering that results in the $A_2BB'O_{6-\delta}$ double perovskite; (3) fluorination of either $A_2BB'O_5$ by fluorine insertion or $A_2BB'O_{6-\delta}$ by $O^{2-} \rightarrow 2F^-$ replacement, resulting in the $A_2BB'(O,F)_6$ layered perovskite-type oxyfluorides.

Anion insertion into the brownmillerite structure can occur in different ways. Anion vacancies can be filled in some of the B′O□ tetrahedral layers, leaving other layers unaffected. Most often, oxygen insertion occurs in every second tetrahedral layer, which changes the...OTOT... brownmillerite layer sequence to...OOOTOOOT... (where O stands for the octahedral BO_2 or $B'O_2$ layer and T for the tetrahedral B′O□ layer). Thus, half of the B′ cations acquire CN = 6 and another half retain the tetrahedral coordination with CN = 4, which corresponds to the $A_2BB'O_{5.5}$ composition. The obtained structure and chemical composition $A_4(B_2B')_{oct}B'_{tetr}O_{11} = 2\cdot A_2BB'O_{5.5}$ corresponds to the $n = 4$ member of the $A_nB_{n-1}B'O_{3n-1}$ brownmillerite homologue series (Figure 3a). A second possibility arises if every B′O□ tetrahedral layer is affected by anion insertion, which causes an increase of the average coordination number of all B′ cations to CN = 5 (in $A_2BB'O_{5.5}$) or 6 (in $A_2BB'(O,F)_6$) (Figure 3b). The anion insertion path depends mostly on the size of the A cations. The brownmillerites with smaller A cations (Ca^{2+}) usually adopt extra anions by changing the O and T layer sequence, as occurs in $Ca_2GaMnO_{5.39}$ and $Ca_2AlMnO_{5.5}$, where the presence of the...OOOTOOOT...

(20) Abakumov, A. M.; Rozova, M. G.; Pavlyuk, B. Ph.; Lobanov, M. V.; Antipov, E. V.; Lebedev, O. I.; Van Tendeloo, G.; Sheptyakov, D. V.; Balagurov, A. M.; Bouree, F. *J. Solid State Chem.* **2001**, *158*, 100–111.

(21) Abakumov, A. M.; Rozova, M. G.; Pavlyuk, B. Ph.; Lobanov, M. V.; Antipov, E. V.; Lebedev, O. I.; Van Tendeloo, G.; Ignatchik, O. L.; Ovtchenkov, E. A.; Koksharov, Yu. A.; Vasi'ev, A. N. *J. Solid State Chem.* **2001**, *160*, 353–361.

(22) Wright, A. J.; Palmer, H. M.; Anderson, P. A.; Greaves, C. *J. Mater. Chem.* **2002**, *12*, 978–982.

(23) Wright, A. J.; Palmer, H. M.; Anderson, P. A.; Greaves, C. *J. Mater. Chem.* **2001**, *11*, 1324–1326.

(24) Battle, P. D.; Bell, A. M.; Blundell, S. J.; Coldea, A. I.; Gallon, D. J.; Pratt, F. L.; Rosseinsky, M. J.; Steer, C. A. *J. Solid State Chem.* **2002**, *167*, 188–195.

(25) Hadermann, J.; Abakumov, A. M.; D'Hondt, H.; Kalyuzhnaya, A. S.; Rozova, M. G.; Markina, M. M.; Mikheev, M. G.; Tristan, N.; Klingeler, R.; Büchner, B.; Antipov, E. V. *J. Mater. Chem.* **2007**, *17*, 692–698.

(26) Cussen, E. J.; Rosseinsky, M. J.; Battle, P. D.; Burley, J. C.; Spring, L. E.; Vente, J. F.; Blundell, S. J.; Coldea, A. I.; Singleton, J. *J. Am. Chem. Soc.* **2001**, *123*, 1111–1122.

(27) Coldea, A. I.; Blundell, S. J.; Marshall, I. M.; Steer, C. A.; Singleton, J.; Pratt, F. L.; Noailles, L. D.; Rosseinsky, M. J.; Spring, L. E.; Battle, P. D. *Phys. Rev.* **2001**, *B65*, 054402.

(28) Battle, P. D.; Blundell, S. J.; Claridge, J. B.; Coldea, A. I.; Cussen, E. J.; Noailles, L. D.; Rosseinsky, M. J.; Singleton, J.; Sloan, J. *Chem. Mater.* **2002**, *14*, 425–434.

(29) Caspi, E. N.; Avdeev, M.; Short, S.; Jorgensen, J. D.; Dabrowski, B.; Chmaissem, O.; Mais, J.; Kolesnik, S. *J. Solid State Chem.* **2004**, *177*, 1456–1470.

(30) Anderson, M. T.; Poeppelmeier, K. R. *Chem. Mater.* **1991**, *3*, 476–482.

(31) Azuma, M.; Kaimori, S.; Takano, M. *Chem. Mater.* **1998**, *10*, 3124–3130.

(32) Abakumov, A. M.; Rossell, M. D.; Seryakov, S. A.; Rozova, M. G.; Markina, M. M.; Van Tendeloo, G.; Antipov, E. V. *J. Mater. Chem.* **2005**, *15*, 4899–4905.

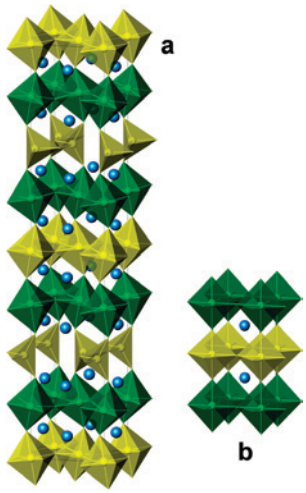

Figure 3. (a) Crystal structure of the $A_4(B_2B')_{oct}B'_{tetr}O_{11}$ member of the brownmillerite homologue series. (b) Crystal structure of the $A_2BB'(O,F)_6$ double perovskite. The B_{oct} cations are in green octahedra, and the B'_{oct} and B'_{tetr} cations are in yellow octahedra and tetrahedra, respectively. The A cations are shown as spheres.

layer sequence was found using high-resolution electron microscopy and neutron powder diffraction, respectively.[20,33] If the A position is occupied by a relatively large cation (Sr^{2+} or Ba^{2+}), the anion insertion occurs according to the second scenario ($LaSrCuGaO_{5-x}F_{2x}$,[34] $Sr_2GaMnO_{5.5}$,[21,35−37] $Sr_2GaMnO_{5-x}F_{1+x}$,[38] $(Ba_{1-x}La_x)_2In_2O_{5+x}$,[39] and $BaIn_{1-x}Ti_xO_{2.5+x/2}$[40]). One could expect that the tendency of the brownmillerite structure to adopt one of these ways of anion insertion would be related to the crystallographic properties of the B′ cations, particularly to their ability to adopt CN = 5. However, a comparison of anion insertion into the $A_2B'MnO_5$ (A = Ca, Sr; B′ = Al, Ga) brownmillerites reflects that the nature of the B′ cation is not a primary reason. A possible explanation can be found in the significantly different crystallographic consequences of two different ways of anion insertion.

If unaffected tetrahedral layers remain, the structure retains orthorhombic symmetry due to ordering of anion vacancies in these layers along the $[110]_p$ rows. Two crystallographically different A positions exist in this structure. The position A1 is located between the BO_2 and B′O□ layers; its oxygen coordination is virtually identical with that of the A position in the brownmillerite structure (eight short and two long A−O distances). The position A2 is sandwiched between the BO_2 and $B'O_2$ layers in a 12-coordinated cavity, as in the ABO_3 perovskite. The coordination number of a small A2 cation (Ca^{2+}) can be reduced to 9 + 3 by cooperative tilts of the BO_6 and $B'O_6$ octahedra. Thus, the $A_4(B_2B')_{oct}B'_{tetr}O_{11}$ structure is suitable for accommodation of the A cations of small size.

In contrast to this orthorhombic structure, oxygen insertion into all anion-deficient layers destroys long-range ordering of anions and vacancies. Increasing the anion content from $A_2BB'O_5$ to $A_2BB'O_{5.5}$ can occur through a slightly orthorhombically distorted phase with $a = a_p\sqrt{2}$, $c = 2a_p$, and *Cmmm* space symmetry and finally leads to a tetragonal double perovskite with $a = a_p$ and $c = 2a_p$ with *P*4/*mmm* space symmetry. The doubling of the perovskite unit cell along the *c* axis reflects the layered ordering of the B and B′ cations and remaining anion vacancies that reside in the $B'O_{2-\delta}$ layers. The lattice parameters and space symmetry imply the absence of a tilting distortion of the octahedral layers, and anion insertion should increase the coordination number of the A cations from 8 + 2 in the initial brownmillerite to 11 (in average) in the tetragonal $A_2BB'O_{5.5}$ double perovskite, which favors the larger size of the A cation.

In both orthorhombic *Cmmm* and tetragonal *P*4/*mmm* double perovskites, the $B'O_{2-\delta}$ layers demonstrate strong disorder of O atoms and vacancies. When the composition of the layer is close to $B'O_{1.5}$, the average coordination number of the B′ cations should be close to 5, but little is known about their exact coordination. Intuitively, this disorder was ascribed to randomly distributed $B'O_4$ tetrahedra and $B'O_6$ octahera, which was also indirectly supported by a general opinion about unfavorable 5-fold coordination for such cations as Ga^{3+}.[29] However, CN = 5 is not something exotic for Ga^{3+}, and several examples of the structures can be found where Ga^{3+} is situated in a trigonal bipyramid: $YGaO_3$,[41] Ga_3PO_7,[42] $RGaGe_2O_7$ (R = Nd, Gd),[43,44] and $GaInO_3$.[45] An analysis of the local coordination using the bond valence sum (BVS) supports that in the $Sr_2GaMnO_{5.5}$[36] and $(Ba_{1-x}La_x)_2In_2O_{5+x}$[39] compounds the Ga^{3+} and In^{3+} cations are situated in the 5-fold polyhedra. CN = 5 for these cations provides BVS values close to the nominal valence, whereas CN = 4 and 6 correspond to strong underbonding and overbonding, respectively. Local ordering of O atoms and vacancies in $Sr_2GaMnO_{5.41}$, compatible with a net of corner-sharing GaO_5 trigonal bipyramids, was also deduced from electron diffraction data (Figure 4a).[36,37]

However, the coexistence of the polyhedra with CN = 4 and 6 becomes possible if the B′ cations with stable tetrahedral coordination (Al^{3+}) are diluted by the octahedrally coordinated cations (Mn^{4+}). In the $Sr_2Al_{0.78}Mn_{1.22}O_{5.2}$ tet-

(33) Palmer, H. M.; Snedden, A.; Wright, A. J.; Greaves, C. *Chem. Mater.* **2006**, *18*, 1130–1133.
(34) Hadermann, J.; Van Tendeloo, G.; Abakumov, A. M.; Pavlyuk, B. Ph.; Rozova, M.; Antipov, E. V. *Int. J. Inorg. Mater.* **2000**, *2*, 493–502.
(35) Pomyakushin, V. Yu.; Balagurov, A. M.; Elzhov, T. V.; Sheptyakov, D. V.; Fisher, P.; Khomskii, D. I.; Yushankhai, V. Yu.; Abakumov, A. M.; Rozova, M. G.; Antipov, E. V.; Lobanov, M. V.; Billinge, S. J. L. *Phys. Rev.* **2002**, *B66*, 184412.
(36) Abakumov, A. M.; Rozova, M. G.; Alekseeva, A. M.; Kovba, M. L.; Antipov, E. V.; Lebedev, O. I.; Van Tendeloo, G. *Solid State Sci.* **2003**, *5*, 871–882.
(37) Antipov, E. V.; Abakumov, A. M.; Alekseeva, A. M.; Rozova, M. G.; Hadermann, J.; Lebedev, O. I.; Van Tendeloo, G. *Phys. Status Solidi A* **2004**, *201*, 1403–1409.
(38) Alekseeva, A. M.; Abakumov, A. M.; Rozova, M. G.; Antipov, E. V.; Hadermann, J. *J. Solid State Chem.* **2004**, *177*, 731–738.
(39) Liu, Y.; Withers, R. L.; Fitz Gerald, J. *J. Solid State Chem.* **2003**, *170*, 247–254.
(40) Jayaraman, V.; Magrez, A.; Caldes, M.; Joubert, O.; Ganne, M.; Piffard, Y.; Brohan, L. *Solid State Ionics* **2004**, *170*, 17–24.
(41) Geller, S.; Jeffries, J. B.; Curlander, P. J. *Acta Crystallogr.* **1975**, *B31*, 2770–2774.
(42) Boudin, S.; Lii, K.-H. *Acta Crystallogr.* **1998**, *C54*, 5–7.
(43) Jarchow, O.; Klaska, K. H. *Z. Kristallogr.* **1985**, *172*, 159–166.
(44) Kaminskii, A. A.; Mill, B. V.; Butashin, A. V.; Belokoneva, E. L.; Kurbanov, K. *Phys. Status Solidi A* **1987**, *103*, 575–592.
(45) Shannon, R. D.; Prewitt, C. T. *J. Inorg. Nucl. Chem.* **1968**, *30*, 1389–1398.

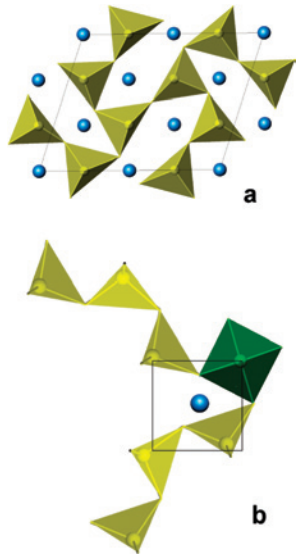

Figure 4. Possible atomic arrangements in the $B'O_{1+\delta}$ layers: (a) B′ cations adopt CN = 5; a monoclinic supercell is outlined; (b) B′ cations adopt CN = 4 and 6; a perovskite subcell is outlined.

ragonal double perovskite ($a = a_p$, $c = 2a_p$, space group *P4/mmm*), the local structure of the disordered $(Al_{0.78}Mn_{0.22})O_{1.2}$ layers can be interpreted as consisting of fragments of brownmillerite-type tetrahedral chains of corner-sharing AlO_4 tetrahedra interrupted by MnO_6 octahedra, at which the chain fragments rotate over 90°, resulting in the average tetragonal symmetry (Figure 4b).

Extra anion insertion can occur under fluorination of the brownmillerites and their anion-excessive $A_2BB'O_{5.5}$ derivatives. The examples of fluorination of $LaACuGaO_5$ (A = Ca, Sr) and $Sr_2GaMnO_{5.5}$ with XeF_2 as a fluorinating agent at 300−600 °C were described.[34,38] Fluorination occurs according to a combined anion exchange/insertion reaction:

$$LaACuGaO_5 + xXeF_2 \rightarrow LaACuGaO_{5-x}F_{2x} + x[O] + xXe$$

$$Sr_2GaMnO_{5.5} + (1+x)/2XeF_2 \rightarrow Sr_2GaMnO_{5-x}F_{1+x} + (1/2+x)[O] + (1+x)/2Xe$$

Thus, the complete filling of anion vacancies can be achieved, as was found in $Sr_2GaMnO_{4.78}F_{1.22}$. It should be noted that such a double perovskite with layered ordering of the cations in the B sublattice could not be prepared by a direct solid-state reaction and was obtained as a result of oxidation and fluorination reactions performed at low-temperature conditions.

Increasing the anion content in the $B'O_{2-\delta}$ layers also affects the bond lengths in the BO_6 (B = Jahn−Teller cation) octahedra in the neighboring layers. Oxygen insertion in A_2GaMnO_5 (A = Ca, Sr; B′ = Al, Ga) causes significant shrinking of the apical Mn−O distance due to suppression of the Jahn−Teller distortion on going from Mn^{3+} to Mn^{4+}. The octahedral distortion parameter $\Delta d = (1/6)\sum_{n=1-6}[(d_n - d)/d]^2$, which characterizes the degree of Jahn−Teller deformation,[46] decreases from 9.95×10^{-3} to 1.87×10^{-4} on going from Sr_2GaMnO_5 to $Sr_2GaMnO_{5.5}$[35] and from 6.74×10^{-3} to 2.66×10^{-3} on going from Ca_2AlMnO_5 to $Ca_2AlMnO_{5.5}$ (in the last case, a rather small decrease of Δd is due to strong off-center displacement of the Mn^{4+} cations).[33] One can expect that the formation of the $Sr_2GaMnO_{5-x}F_{1+x}$ solid solutions, accompanied by a reduction of the Mn cations, would restore the Jahn−Teller apical distortion. However, in $Sr_2GaMnO_{4.78}F_{1.22}$ ($V_{Mn} = +3.78$) even slight apical compression of the MnO_6 octahedra was observed [$d(Mn-O_{eq}) = 1.928$ Å; $d(Mn-O_{ap}) = 1.876$ Å].[38] It was assumed that the reversed sign of the Jahn−Teller distortion arises from an interplay between a free energy decrease from deformation of the MnO_6 octahedra and simultaneous variation of the electrostatic lattice energy due to changes in the Sr−(O,F) bond distances. In the oxygen-doped $Sr_2MnGaO_{5+\delta}$ compounds, the apical elongation of the MnO_6 octahedra upon reduction is accompanied by a shortening of the Ga−O_{ap} distance due to a decrease of the coordination of Ga down to 4 (Figure 5).[36] For the $Sr_2MnGaO_{5-x}F_{1+x}$ solid solutions, the Ga−O_{ap} distance does not vary because the amount of anions and the CN of the Ga atoms is constant. If the reduction of the Mn cations is accompanied by an elongation of the Mn−O_{ap} distances, it would result in abnormally long Sr−(O,F) separations, followed by a decrease of the lattice energy.[38]

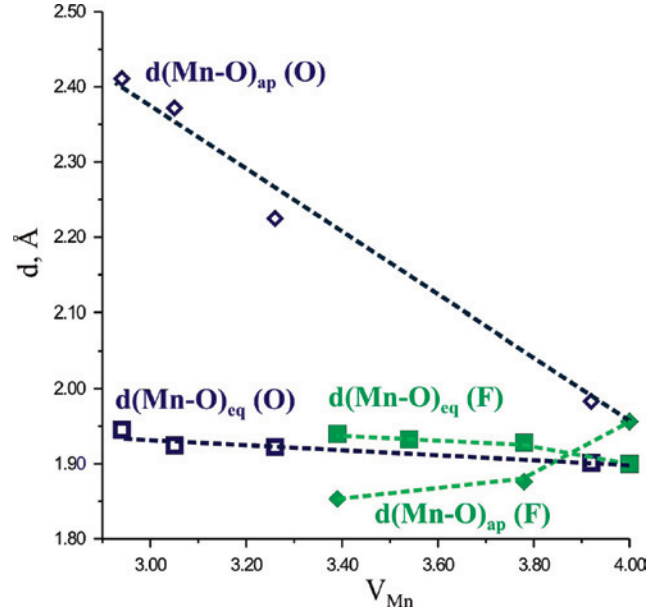

Figure 5. Equatorial and apical Mn−(O,F) distances in the oxygen-doped $Sr_2MnGaO_{5+\delta}$ (O) and fluorine-doped $Sr_2MnGaO_{5-x}F_{1+x}$ (F) as a function of V_{Mn}.

Changing the anion content on going along the sequence Sr_2GaMnO_5−$Sr_2GaMnO_{5.5}$−$Sr_2GaMnO_{4.78}F_{1.22}$ does not directly affect the magnetically active MnO_2 layers, except changing the Mn oxidation state. However, variation of the anion content in the magnetically inactive Ga layers modifies significantly the magnetic ordering pattern in these materials.[47] The Sr_2GaMnO_5 brownmillerite demonstrates G-type antiferromagnetic (AFM) ordering below $T_N = 180-183$ K; i.e., the magnetic moment on the Mn atoms are coupled

(46) Alonso, J. A.; Martinez-Lope, M. J.; Casais, M. T.; Fernandez-Diaz, M. T. *Inorg. Chem.* **2000**, *39*, 917–923.

(47) Abakumov, A. M.; Rozova, M. G.; Antipov, E. V. *Russ. Chem. Rev.* **2004**, *73*, 847–860.

antiferromagnetically between the nearest neighbors within MnO_2 and between the adjacent MnO_2 planes.[29,35] Inserting extra O atoms into the Ga layers in $Sr_2GaMnO_{5.5}$ creates a competing diagonal 180° superexchange path between the Mn^{4+} cations in the adjacent layers through the $GaO_{1.5}$ layers, which results in a C-type AFM magnetic structure (T_N = 110 K) where the magnetic moments on the Mn atoms remain antiparallel in the MnO_2 layers but become ferromagnetically coupled between two neighboring MnO_2 layers.[29,35] The magnetic moments in both compounds are aligned along the stacking axis of the Mn and Ga layers, in agreement with the orbital $3d_{3z^2-r^2}$ ordering. Slight apical compression of the MnO_6 octahedra in $Sr_2GaMnO_{4.78}F_{1.22}$ is accompanied by a magnetically ordered state below T_N = 70 K with the magnetic moments on the Mn atoms aligned parallel to the MnO_2 planes where they form ferromagnetic rods along $[100]_p$, which are AFM-coupled along $[010]_p$ (in agreement with the tetragonal to orthorhombic phase transition at T_c = 150 K); the neighboring MnO_2 layers are stacked ferromagnetically.[48] Because of V_{Mn} = +3.78, this type of magnetic structure can be governed by simultaneously present superexchange interactions and double Mn^{3+}−O−Mn^{4+} exchange and might be related to a change of the orbital ordering type from $3d_{3z^2-r^2}$ to $3d_{x^2-y^2}$.

4. Coupled A Site and Anion Vacancy Ordering in Anion-Deficient Perovskites

Up to now, anion insertion into the brownmillerite structure has been discussed without particular attention to the A sublattice, assuming that the A positions are occupied by a single cation type or by two A cations with close sizes in a random way. Indeed, the $A_2BB'O_5$ brownmillerite structure contains only one type of cavity available for the A cations, and an attempt to insert two A cations with significantly different sizes and characteristic coordination numbers can result in a change in the oxygen/vacancy pattern due to coupled A cation and anion ordering. One can consider two homologue series $A_nB_{n-1}B'O_{3n-1}$ and $A_{n-1}A'B_nO_{3n-1}$, where divalent alkali-earth and trivalent rare-earth cations are located in the A sublattice. The $A_nB_{n-1}B'O_{3n-1}$ series was already mentioned above; it is the brownmillerite homologue series where the perovskite blocks with average thicknesses of $n - 1$ octahedra are separated by anion-deficient B′O□ layers. In the $A_{n-1}A'B_nO_{3n-1}$ compounds, because of the smaller sizes of A′ cations in comparison with that of the A cations, the anion vacancies are concentrated in the A′□ layers, so that the B cations in the adjacent BO_2 layers acquire tetragonal pyramidal coordination. Thus, the layer sequences for both series can be written as

$A_nB_{n-1}B'O_{3n-1}$: −B′O−AO−BO_2−[AO−BO_2]$_{n-2}$−AO−B′O−

$A_{n-1}A'B_nO_{3n-1}$: −A′−[BO_2−AO]$_{n-1}$−BO_2−A′

One of the driving forces for the layered ordering in $A_{n-1}A'B_nO_{3n-1}$ in comparison with the brownmillerite-type $A_nB_{n-1}B'O_{3n-1}$ compounds is a significant difference in the coordination numbers of the A and A′ cations. In the $BaRFe_2O_5$[49−51] and $Ba_2RFe_3O_{8+\delta}$[52−55] compounds, the rare-earth cations A′ (R = Y) and alkali-earth cations A (Ba) have CNs of 8 and 12, respectively. An important influence of the anion vacancy ordering on the A-site ordering can be shown using an example of the $BaLaMn_2O_{6-\delta}$ (δ = 0, 1) compounds.[56,57] The $BaLaMn_2O_6$ compound with a complete anion sublattice demonstrates no order between Ba^{2+} and La^{3+} cations. However, the synthesis of anion-deficient $BaLaMn_2O_5$ results in the layered ordering of anion vacancies and the A cations, as was found in $BaRFe_2O_5$. Subsequent soft oxidation allows preservation of the A-site ordering in the stoichiomentric $BaLaMn_2O_6$ perovskite.

One can expect that the ordered stacking of layers in the homologues of both $A_{n-1}A'B_nO_{3n-1}$ and $A_nB_{n-1}B'O_{3n-1}$ series will become less stable with increasing n, i.e., with increasing distance between the anion-deficient layers and decreasing amounts of oxygen vacancies. Because of the repulsive forces between positively charged vacancies, they tend to be more homogeneously distributed in the structure, which raises difficulties in obtaining ordered layer sequences. The ordering in the n = 4−6 $A_{n-1}A'B_nO_{3n-1}$ compounds is achieved if it is assisted by concomitant order of two B cations with stable CN = 5 and 6, as was observed in the mixed oxides $(AA'Cu_2O_5)(ABO_3)_{n-2}$ (B = Ti, Sn).[58−60] Starting from a certain n value, it becomes more profitable to increase the coordination number of the cations in the anion-deficient layers rather than to increase the thickness of the perovskite block between the anion-deficient layers.

Attempts to introduce extra oxygen into the anion-deficient $Sr_2Co_2O_5$ perovskite by heterovalent replacement of Sr^{2+} by R^{3+} results in a new ordering pattern of anion vacancies coupled with the ordering at the A sublattice. The anion-deficient cobaltites $(Sr,R)CoO_{2.5+\delta}$ ($Sr_{0.7}Y_{0.3}CoO_{2.62}$,[61] $Sr_{0.7}Dy_{0.3}CoO_{2.62}$,[62] $Sr_{0.66}Y_{0.33}CoO_{2.79}$,[63] $Sr_xR_{1-x}CoO_{3-y}$, R =

(48) Pomjakushin, V.; Sheptyakov, D.; Fischer, P.; Balagurov, A.; Abakumov, A.; Alekseeva, A.; Rozova, M.; Antipov, E. *Physica B: Condens. Matter* **2004**, *350*, E23−E26.

(49) Karen, P.; Woodward, P. M.; Linden, J.; Vogt, T.; Studer, A.; Fischer, P. *Phys. Rev. B: Condens. Matter Mater. Phys.* **2001**, *64*, 214405/1–214405/14.

(50) Woodward, P. M.; Karen, P. *Inorg. Chem.* **2003**, *42*, 1121–1129.

(51) Woodward, P. M.; Suard, E.; Karen, P. *J. Am. Chem. Soc.* **2003**, *125*, 8889–8899.

(52) Karen, P.; Kjekshus, A.; Huang, Q.; Karen, V. L.; Lynn, J. W.; Rosov, N.; Sora, I. N.; Santoro, A. *J. Solid State Chem.* **2003**, *174*, 87–95.

(53) El Massalami, M.; Elzubair, A.; Ibrahim, H. M.; Rizgalla, M. A. *Physica C* **1991**, *183*, 143–148.

(54) Huang, Q.; Karen, P.; Karen, V. L.; Kjekshus, A.; Lynn, J. W.; Mighell, A. D.; Rosov, N.; Santoro, A. *Phys. Rev.* **1992**, *B45*, 9611–9619.

(55) Karen, P.; Kjekshus, A.; Huang, Q.; Lynn, J. W.; Rosov, N.; Sora, I. N.; Karen, V. L.; Mighell, A. D.; Santoro, A. *J. Solid State Chem.* **1998**, *136*, 21–33.

(56) Caignaert, V.; Millange, F.; Domenges, B.; Raveau, B.; Suard, E. *Chem. Mater.* **1999**, *11*, 930–938.

(57) Millange, F.; Caignaert, V.; Domenges, B.; Raveau, B.; Suard, E. *Chem. Mater.* **1998**, *10*, 1974–1983.

(58) Gormezano, A.; Weller, M. T. *J. Mater. Chem.* **1993**, *3*, 771–772.

(59) Anderson, M. T.; Poeppelmeier, K. R.; Zhang, J.-P.; Fan, H.-J.; Marks, L. D. *Chem. Mater.* **1992**, *4*, 1305–1313.

(60) Otzschi, K. D.; Vander Griend, D. A.; Poeppelmeier, K. R.; Sinkler, W.; Marks, L. D.; Mason, T. O. *Chem. Mater.* **1998**, *10*, 2579–2581.

(61) Istomin, S. Ya.; Grins, J.; Svensson, G.; Drozhzhin, O. A.; Kozhevnikov, V. L.; Antipov, E. V.; Attfield, J. P. *Chem. Mater.* **2003**, *15*, 4012–4020.

(62) Istomin, S. Ya.; Drozhzhin, O. A.; Svensson, G.; Antipov, E. V. *Solid State Sci.* **2004**, *6*, 539–546.

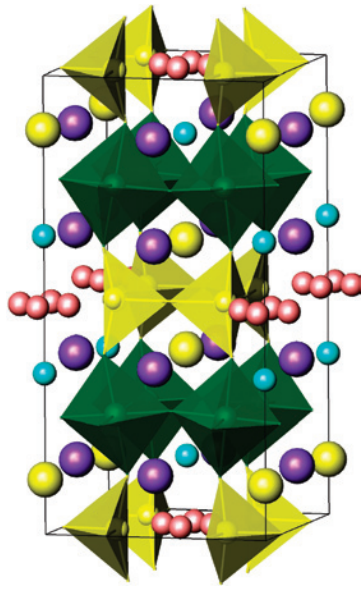

Figure 6. Crystal structure of $Sr_{0.7}Y_{0.3}CoO_{2.62}$. The Sr cations are shown as large yellow and blue spheres and the R cations as smaller cyan spheres. The disordered oxygen position (O4) is shown as red spheres. The Co cations are situated in the octahedra (green) and tetrahedra (yellow).

Sm−Yb, Y; $0.6 < x \leq 0.9$[64]) as well as the $Sr_{0.73}Y_{0.27}Mn_{0.67}Ga_{0.33}O_{2.63}$ manganite[65] do not contain the A′□ layers, as the $A_{n-1}A'B_nO_{3n-1}$ structures. The crystal structure of the Co-based compounds (Figure 6) is tetragonal (space group *I*4/*mmm*) with $a \approx 2a_p$ and $c \approx 4a_p$ and contains layers of tilted CoO_6 octahedra that alternate with the oxygen-deficient layers according to the $-CoO_2-(Sr,R)O-CoO_{1+2\delta}-(Sr,R)O-CoO_2-$ sequence. The $CoO_{1+2\delta}$ layer consists of clusters of four CoO_4 tetrahedra, where each tetrahedron shares two O atoms with the adjacent tetrahedra. An extra O atom (marked as O4 in Figure 7a), located between four tetrahedral clusters, expands the coordination of a fraction of the Co atoms in these layers up to CN = 4 + 1 (four shorter and one longer Co−O separations).

The idealized position of these extra O atoms would be at the middle of the edge of the perovskite subcell, as is shown in Figure 7b for the O5 atom. Changing the oxygen amount in the anion-deficient layers and the size of the rare-earth cation is accompanied by a displacement of the extra O atom from the edge toward the face center of the perovskite subcell (O4 in Figure 7a,b). In the last case, the occupancy of the O4 position cannot exceed 25% in order to avoid short O−O separations, which corresponds to maximal $\delta = 0.125$ and equal amounts of the CoO_4 tetrahedra and CoO_5 polyhedra in the anion-deficient layers. The location of the extra O atom near the center of the face of the perovskite subcell provides typical bonding distances from this atom to the small rare-earth cations above and below what is naturally associated with

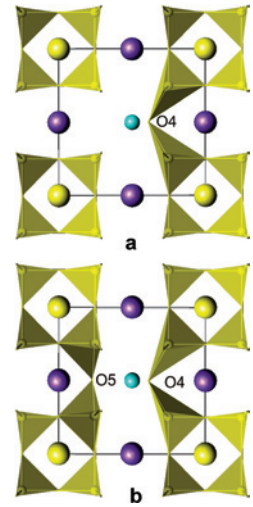

Figure 7. Two possible atomic arrangements in the anion-deficient $CoO_{1+2\delta}$ layers: (a) only the O4 atoms are present; (b) both O4 and O5 atoms are present.

the A-cation ordering, such as, for example, in $Sr_{0.7}Dy_{0.3}CoO_{2.62}$[62] or $Sr_{0.73}Y_{0.27}Mn_{0.67}Ga_{0.33}O_{2.63(1)}$.[65]

For compounds with $\delta > 0.125$, where the A cations ($Sr_{0.67}Ho_{0.33}CoO_{3-y}$, $y = 0.33, 0.29, 0.20$[66] and $Sr_{0.75}Y_{0.25}Co_{0.5}Fe_{0.5}O_{2.69(2)}$[67]) are ordered, the maximal occupancy of the O4 position is 25% and further oxygen insertion occurs in the position O5. Avoiding the short O4−O5 distance requires that the 4-fold O5 position only be occupied by 25%, i.e., one O5 atom out of four is present in the layer. In the case of such a joint occupation of the O4 and O5 positions, all Co atoms in the layer are 5-fold-coordinated (Figure 7b), which corresponds to $\delta = 0.25$. An increase of the oxygen content up to $\delta = 0.3$ was also reported that might be related to cooperative displacements of the O atoms, which optimize the O−O distances.[66]

In the compounds with no A-cation ordering due to small size difference ($Sr_{0.67}La_{0.33}CoO_{2.72}$[68] and $Sr_{1-x}Bi_xCoO_{3-y}$, $x = 0.1, 0.1, 0.2$;[69] $r(Sr^{2+}) = 1.25$ Å, $r(La^{3+}) = 1.18$ Å, and $r(Bi^{3+}) = 1.11$ Å; CN = 8 [70]), the O atoms occupy solely the O5 position, leaving the O4 position vacant. The A−O5 distance is larger than the A−O4 one, which is consistent with the absence of the A-cation ordering. However, one should note that the structure refinement from powder X-ray or neutron diffraction data must be necessarily combined with electron diffraction investigation. The absence of electron diffraction data for $Sr_{0.67}La_{0.33}CoO_{2.72}$[68] raises doubts in the choice of the unit cell and space group, which probably explains physically meaningless thermal parameters of the O atoms obtained in the NPD refinement for this compound.

(63) Withers, R. L.; James, M.; Goossens, D. J. *J. Solid State Chem.* **2003**, *174*, 198–208.
(64) James, M.; Cassidy, D.; Goossens, D. J.; Withers, R. L. *J. Solid State Chem.* **2004**, *177*, 1886–1895.
(65) Gillie, L. J.; Palmer, H. M.; Wright, A. J.; Hadermann, J.; Van Tendeloo, G.; Greaves, C. *J. Phys. Chem. Solids* **2004**, *65*, 87–93.
(66) Baszczuk, A.; Kolesnik, S.; Dabrowski, B.; Chmaissem, O.; Mais, J. *Phys. Rev.* **2007**, *B76*, 134407.
(67) Lindberg, F.; Drozhzhin, O. A.; Istomin, S. Ya.; Svensson, G.; Kaynak, F. B.; Svedlindh, P.; Warnicke, P.; Wannberg, A.; Mellergård, A.; Antipov, E. V. *J. Solid State Chem.* **2006**, *179*, 1433–1443.
(68) Kolesnik, S.; Dabrowski, B.; Mais, J.; Majjiga, M.; Chmaissem, O.; Baszczuk, A.; Jorgensen, J. D. *Phys. Rev.* **2006**, *B73*, 214440.
(69) Knee, Ch. S.; Lindberg, F.; Khan, N.; Svensson, G.; Svedlindh, P.; Rundlöf, H.; Eriksson, S. G.; Börjesson, L. *Chem. Mater.* **2006**, *18*, 1354–1364.
(70) Shannon, R. D. *Acta Crystallogr.* **1976**, *A32*, 751–767.

5. Crystallographic Shear Structures in Anion-Deficient Perovskites

Heterovalent substitution in the A sublattice of brownmillerites followed by increasing oxygen content can result either in disordered anion-deficient layers ($(Ba_{1-x}La_x)_2In_2O_{5+x}$[39]) or in the appearance of another type of ordered pattern due to coupling with A-cation ordering (as in the $(Sr,R)CoO_{2.5+\delta}$ phases). One can expect that an isovalent substitution at the A sublattice would not result in drastic structural changes because it is not accompanied by anion insertion and does not affect directly the anion-deficient layers. However, this remains valid unless the A cations do not differ significantly in their electronic structure. For instance, there exist numerous $A_2BB'O_5$ brownmillerites with A = Sr, but the brownmillerites with Pb^{2+} in the A position have not been observed even in spite of close ionic radii ($r(Sr^{2+})$ = 1.25 Å; $r(Pb^{2+})$ = 1.29 Å; CN = 8[70]). According to analysis of the BVS, the A-site cavity in the $Sr_2Fe_2O_5$ brownmillerite is equally suitable for both Sr^{2+} (BVS = +2.09) and Pb^{2+} (BVS = +2.10) cations. Cations such as Pb^{2+} and Bi^{3+} can be accommodated at the A positions of the perovskite structure ($BiFeO_3$,[71] $PbFeO_2F$,[72] and $PbVO_3$ [73]), where they often demonstrate clear stereochemical activity of the localized lone $6s^2$ electron pair. It is reflected by strong tetragonal polar distortion in $PbVO_3$[73] or by random off-center displacements of the Pb^{2+} cations along the ⟨110⟩ directions in $PbFeO_2F$.[72] One could expect that the brownmillerite structure should also be able to accommodate such A cations, but the crystal structure of the $(Pb,A)_2Fe_2O_5$ (A = Sr, Ba) perovskites is significantly modified in order to accommodate the lone-pair domains. The $Pb_{1.33}Sr_{0.67}Fe_2O_5$ compound has the same $A_2BB'O_5$ stoichiometry as brownmillerite and the orthorhombic unit cell clearly related to the perovskite subcell as $a \approx \sqrt{2}a_p$, $b \approx a_p$, and $c \approx 4\sqrt{2}a_p$.[74] The structure consists of a sequence of parallel perovskite blocks shaped by the $(\bar{1}01)_p$ perovskite planes and alternating along the *c* axis (Figure 8). The thickness of the blocks is two FeO_6 octahedra, and the blocks are displaced with respect to each other by the $^1/_2[110]_p$ vector. The blocks are linked together by infinite chains of edge-sharing distorted FeO_5 tetragonal pyramids running along the *b* axis. Between two successive chains, the six-sided tunnels are formed. The A cations are located in the cavities of the perovskite blocks and also as double columns inside the six-sided tunnels. The A cations in the tunnels have an asymmetric coordination environment with three shorter A−O distances (2.28−2.43 Å) and three longer ones (2.63−2.70 Å). Such a coordination environment is not suitable for the Sr cations. These tunnels are exclusively occupied by the Pb atoms, whereas the A positions in the perovskite blocks are randomly occupied by Sr and the rest of the Pb cations. The necessary condition for the formation of such six-sided tunnels is the presence of an A cation with an asymmetric coordination environment completed by a localized lone electron pair. Another structure requirement is the ability of the B cation to adopt the coordination numbers 5 and 6. Similar, but more complex structures were observed in "$PbMnO_{2.75}$"[75] and "$Pb_2Fe_2O_5$";[76] the latter compound was assumed earlier to have the brownmillerite-type structure.[77] The generalized building principles of these structures can be formulated using a conception of crystallographic shear (CS) planes. From this point of view, the crystal structure is considered as a result of fragmentation of the parent perovskite structure by periodically spaced parallel translational interfaces with the $\mathbf{R} = {}^1/_2[110]_p$ displacement vector applied along the interfaces. A displacement of one part of the perovskite structure with respect to the other changes the connectivity scheme of the B−O polyhedra, resulting in the replacement of the corner-shared BO_6 octahedra by edge-shared tetragonal BO_5 pyramids at the interfaces. The exact structure of the interface depends on its crystallographic orientation: the structures of some low-index $^1/_2[110](\bar{1}01)_p$, $^1/_2[110](100)_p$, and $^1/_2[110](001)_p$ interfaces are shown in Figure 9. More complex interfaces with high $(h0l)_p$ indexes can be formally resolved into a combination of the simple low-index parts. For example, the CS interfaces in the "$Pb_2Fe_2O_5$" sample can be represented as $p\{101\}_p + q\{001\}_p$, which results in a general composition $pPb_2Fe_2O_4 + qPbFe_2O_3 + 2(p+q)PbFeO_3 = Pb_{4p+3q}Fe_{4(p+q)}O_{10p+9q}$, assuming $V_{Fe} = +3$, as confirmed

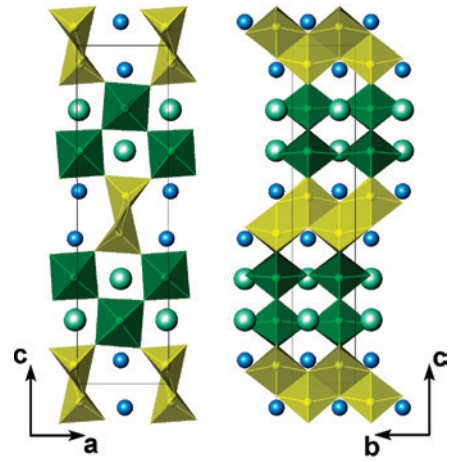

Figure 8. Crystal structure of $Pb_{1.33}Sr_{0.67}Fe_2O_5$. The Fe atoms are located in octahedra (green) and distorted tetragonal pyramids (yellow). The Pb atoms are shown as small blue spheres and the (Pb, Sr) atoms as larger spheres.

(71) Sosnowska, I.; Schaefer, W.; Kockelmann, W.; Andersen, K. H.; Troyanchuk, I. O. *Appl. Phys.* **2002**, *A74*, S1040−S1042.
(72) Inaguma, Y.; Greneche, J.-M.; Crosnier-Lopez, M.-P.; Katsumata, T.; Calage, Y.; Fourquet, J.-L. *Chem. Mater.* **2005**, *17*, 1386–1390.
(73) Shpanchenko, R. V.; Chernaya, V. V.; Tsirlin, A. A.; Chizhov, P. S.; Sklovsky, D. E.; Antipov, E. V.; Khlybov, E. P.; Pomjakushin, V.; Balagurov, A. M.; Medvedeva, J. E.; Kaul, E. E.; Geibel, C. *Chem. Mater.* **2004**, *16*, 3267–3273.
(74) Raynova-Schwarten, V.; Massa, W.; Babel, D. Z. Z. *Anorg. Allg. Chem.* **1997**, *623*, 1048–1054.
(75) Bougerol, C.; Gorius, M. F.; Grey, I. E. *J. Solid State Chem.* **2002**, *169*, 131–138.
(76) Abakumov, A. M.; Hadermann, J.; Bals, S.; Nikolaev, I. V.; Antipov, E. V.; Van Tendeloo, G. *Angew. Chem., Int. Ed.* **2006**, *45*, 6697–6700.
(77) Grenier, J.-C.; Pouchard, M.; Hagenmuller, P. *Rev. Chim. Miner.* **1977**, *14*, 515–522.

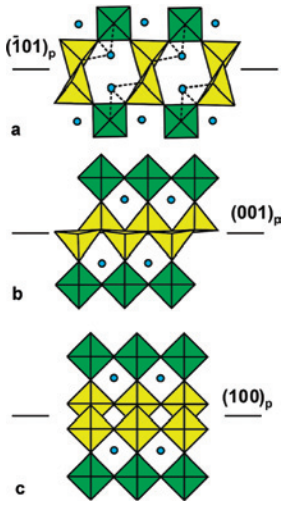

Figure 9. Schematic representation of the structures of the low-index interfaces: (a) $^1/_2[110](\bar{1}01)_p$; (b) $^1/_2[110](001)_p$; (c) $^1/_2[110](100)_p$. The edge-sharing polyhedra are painted in yellow.

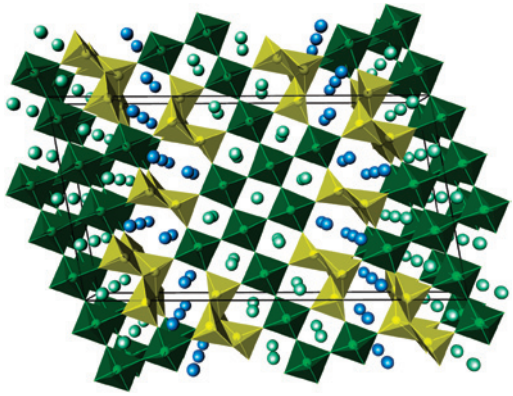

Figure 10. $Pb_{15}Fe_{16}O_{39}$ $^1/_2[110](104)_p$ CS structure. The FeO_5 tetragonal pyramids are yellow, and the Pb atoms in the six-sided tunnels are blue.

by Mössbauer spectroscopy.[77] The CS structures with the $^1/_2[110](104)_p$ (Figure 10), $^1/_2[110](102)_p$, and $^1/_2[110](\bar{3}05)_p$ CS planes were experimentally observed in "$Pb_2Fe_2O_5$" using transmission electron microscopy,[78] but the preparation of these structures in a bulk single-phase form seems to be a challenging problem. Coexisting domains with different $(h0l)_p$ CS planes in "$Pb_2Fe_2O_5$" can be most probably attributed to local cation inhomogeneity, which is difficult to avoid at relatively low synthesis temperature, limiting the cation diffusion. The preferential formation of a particular CS structure and the suppression of other possible variants should require precise control of the cation composition and a decrease of the cation inhomogeneity in the samples. One can expect that advanced techniques of chemical homogenization would result in the successful preparation of such perovskite-like compounds in a pure form. The high-pressure high-temperature technique might be of great help in this case, extending the range of B cations for these types of structures.

(78) Hadermann, J.; Abakumov, A. M.; Nikolaev, I. V.; Antipov, E. V.; Van Tendeloo, G. *Solid State Sci.* **2008**, *10*, 382–389.

6. Conclusions

This review illustrates fruitful approaches for the design of new perovskite-like structures, based on crystal chemistry properties of the A and/or B cations. Introducing two different B cations with distinct coordination numbers into a perovskite structure with an incomplete anion sublattice often results in ordering of the B cations and anion vacancies, leading to the formation of layered structures, such as the $A_2BB'O_5$ brownmillerites. The brownmillerite structure is considered as a starting point for various modifications. By mild-temperature oxidation and/or fluorination, the anion-deficient brownmillerite structure can be converted to a double perovskite $A_2BB'(O,F)_6$ with remaining layered ordering of the B and B′ cations, which cannot be prepared by means of a straightforward high-temperature solid-state reaction. Similarly, coupled A-site and anion vacancy ordering can occur in the anion-deficient perovskites, if the ordering pattern of anion vacancies creates several A sites that can be preferably occupied by A cations with different sizes. Thus, an introduction of small rare-earth cations into the A positions causes a transformation of the brownmillerite structure with a single A-site type into the anion-deficient perovskite containing clusters of four BO_4 tetrahedra and different kinds of A positions suitable to accommodate larger and smaller A cations in an ordered manner. A specific electronic structure of the A cations, such as the presence of a lone $6s^2$ electron pair, results in a transformation of the brownmillerite structure into the perovskite-like structure fragmented by periodic crystallographic shear planes.

These approaches can be used for target-aimed synthesis of the perovskite-like compounds with the required type of cations and anion vacancy ordering, related to requested physical properties. For instance, layered cation ordering creates a quasi-two-dimensional system for charge carrier transfer and for magnetic interactions, which is crucial for various practical applications. High-temperature superconductivity in complex cuprates is proven to be assigned to nearly flat (CuO_2) sheets, properly doped with holes or electrons.[79,80] The layered manganites represent a natural structural matrix for the colossal magnetoresistance (CMR) by the mechanism of tunnelling of the conductivity electrons through the insulating blocks separating the conducting perovskite fragments. The CMR effect in complex oxides $R_{2-x}A_{1+x}Mn_2O_7$ (R = La, Pr, Nd; A = Ca, Sr) stimulated studies of this phenomenon in other manganites with anisotropic layered structures.[81−84] Partial elimination of anion vacancies through

(79) Antipov, E. V.; Abakumov, A. M.; Putilin, S. N. *Supercond. Sci. Technol.* **2002**, *15*, R31−R49.
(80) Antipov, E. V.; Abakumov, A. M. *Phys.-Usp.* **2008**, *51*, 180–190.
(81) Moritomo, Y.; Asamitsu, A.; Kuwahara, H.; Tokura, Y. *Nature* **1996**, *380*, 141–144.
(82) Kimura, T.; Tomioka, Y.; Kuwahara, H.; Asamitsu, A.; Tamura, M.; Tokura, Y. *Science* **1996**, *274*, 1698–1701.
(83) Battle, P. D.; Bell, A. M.; Blundell, S. J.; Coldea, A. I.; Gallon, D. J.; Pratt, F. L.; Rosseinsky, M. J.; Steer, C. A. *J. Solid State Chem.* **2002**, *167*, 188–195.

the formation of the CS planes is closely related to a presence of the A cations with a localized lone electron pair. The CS plane in the perovskite matrix creates chains of edge-sharing BO_5 polyhedra. Thus, the infinite three-dimensional framework of nearly 180° B−O−B exchange interactions becomes periodically interrupted by planes with dominating ~90° exchange interactions, resulting in reduced dimensionality.[85] Such materials can be potential multiferroics due to simultaneous polar distortion caused by the stereochemical activity of a lone electron pair of the A cations and magnetic ordering over the B sublattice.[86]

(84) Battle, P. D.; Blundell, S. J.; Santhosh, P. N.; Rosseinsky, M. J.; Steer, C. *J. Phys.: Condens. Matter* **2002**, *14*, 13569–13577.
(85) Nikolaev, I. V.; D'Hondt, H.; Abakumov, A. M.; Hadermann, J.; Balagurov, A. M.; Bobrikov, I. A.; Sheptyakov, D. V.; Pomjakushin, V. Yu.; Pokholok, K. V.; Filimonov, D. S.; Van Tendeloo, G.; Antipov, E. V. *Phys. Rev. B* **2008**, *78*, 024426.
(86) Khomskii, D. I. *J. Magn. Magn. Mater.* **2006**, *306*, 1–8.

Acknowledgment. This work was supported by the Russian Foundation of Basic Research (Grants 07-03-00664-a, 06-03-90168-à, 05-03-34812-MF-à, and 08-03-00919-a).

IC800791S